Paper:
Xiao, H., Li, Z., Yang, C., Zhang, L., Yuan, P., Ding, L. & Wang, T. (2016). Robust Stabilization of A Wheeled Mobile Robot Using Model Predictive Control Based on Neuro-dynamics Optimization. *IEEE Transactions on Industrial Electronics*, 1-1.
http://dx.doi.org/10.1109/TIE.2016.2606358

Robust Stabilization of A Wheeled Mobile Robot Using Model Predictive Control Based on Neuro-dynamics Optimization

Hanzhen Xiao, Zhijun Li *Senior Member, IEEE*, Chenguang Yang *Senior Member, IEEE*,
Lixian Zhang, Peijiang Yuan, Liang Ding, Tianmiao Wang

***Abstract*—In this paper, a robust model predictive control (MPC) scheme using neural network based optimization has been developed to stabilize a physically constrained mobile robot. By applying a state scaling transformation, the intrinsic controllability of a mobile robots can be regained by incorporation into the control input u_1 an additional exponential decaying term. An MPC based control method is then designed for the robot in the presence of external disturbances. The MPC optimization can be formulated as a convex nonlinear minimization problem and a primal-dual neural network (PDNN) is adopted to solve this optimization problem over a finite receding horizon. The computational efficiency of MPC has been improved by the proposed neuro-dynamic approach. Experimental studies under various dynamic conditions have been performed to demonstrate the performance of the proposed approach.**

***Index Terms*—Robust nonholonomic mobile robots, Scaling transformation, Model predictive control(MPC), Primal-dual neural network (PDNN).**

I. INTRODUCTION

Wheeled mobile robots are playing an important role in social application [1]. Their dynamics under nonholonomic constraints can be formulated into a chained form. However, in accordance to the well known Brockett theorem [2], one cannot apply the differentiable, or even continuous, pure-state feedback to stabilize a nonholonomic systems of motion constraints to a specified posture [3]. Thus, it is generally a challenging task to develop a proper controller to stabilize nonholonomic mobile robots, though much effort from the control community has been devoted to solve these problems.

In recent decades, in order to achieve stabilization or tracking control of the mobile robots, as well as more general nonholonomic chained systems, many methods have been proposed for new development of suitable time-varying controllers. In [4], a receding horizon controller was developed for mobile robot regulation under nonholonomic constraints, by incorporation of a terminal-state region and a terminal-state penalty into the optimization constraints, and the cost function, respectively. In [5], another receding horizon controller was designed for the mobile robot to track a specified trajectory. In [6], a robot formation algorithm based on MPC was presented. To reduce the computational time, a suboptimal stable solution is used in the MPC. In [7], a transverse function based approach is utilized to tracking control of any reference trajectories even fixed-points and non admissible trajectories. In [8], both trajectory tracking and stabilizing to a point have been achieved with exponential convergence rate. To solve the problem of track slipping, in [9], a model perturbation that violates the pure nonholonomic constraints was considered and a feasible solution was developed. For a class of nonholonomic mobile robots, in [10], the saturated practical stabilization problem was addressed based on visual servoing feedback with uncertain camera parameters. The singularity problem caused by the state or input transformation can be avoided by the original system based switching control. In [11], an integral sliding mode controller was developed for the trajectory tracking of a nonholonomic mobile robot, in its inner loop, an improved velocity saturated controller based on hyperbolic tangent function is combined. In [14]–[16], the vector field feedback control approach was proposed for the mobile robot to achieve position stabilization, planned trajectory tracking and obstacles avoidance can be also combined. However, the constrains of states and control input were not considered in the control methods. In [17], an exponential decaying term was integrated into control inputs for driving the system state away from the singular manifold. In [18], by applying the chained form of nonholonomic mobile robot, an additive function explicitly depending on time was incorporated into the input to ensure controllability. However, the above reported works on the stabilization of nonholonomic mobile robots have not considered the internal constraints, including actuator saturation, velocity increment limitation, and boundaries of the robot's dynamics state. Although a variety of approaches stabilizing nonlinear systems under state constraints have been proposed in [19], [20], [21] and [22], where the constraints can be either as non-physical constraints in performance requirements or physical constraints as in actuators, these proposed approach apparently cannot applied to nonholonomic systems.

In the past two decades, MPC has contributed significantly to explicitly optimize the overall performance of control system. In each sampling interval, the control input can be

Manuscript received April 18, 2015; revised September 04, 2015, December 08, 2015, February 14, 2016, April 16, 2016, June 22, 2016; and accepted July 16, 2016. This work is supported in part by National Natural Science Foundation of China grants Nos. 61573147, 91520201, and Guangzhou Research Collaborative Innovation Projects (No. 2014Y2-00507), Guangdong Science and Technology Research Collaborative Innovation Projects under Grant Nos. 2014B090901056, 2015B020214003, Guangdong Science and Technology Plan Project (Application Technology Research Foundation) No. 2015B020233006, and National High-Tech Research and Development Program of China (863 Program) (Grant No. 2015AA042303). *Corresponding author: Zhijun Li (zjli@ieee.org).

H. Xiao and Z. Li are with College of Automation Science and Engineering, South China University of Technology, Guangzhou, 510641, China (email: zjli@ieee.org).

C. Yang is with Zienkiewicz Centre for Computational Engineering, Swansea University, Swansea, SA1 8EN, UK (email: cyang@theiet.org).

L. Zhang and L. Ding are with Research Institute of Intelligent Control and Systems, School of Astronautics, Harbin Institute of Technology, Harbin, 150001, China (email: {liangding, lixianzhang}@hit.edu.cn).

P. Yuan and T. Wang are with the Robotics Institute, Beihang University, Beijing, 100191, China (e-mail: itr@buaa.edu.cn).

obtained by solving a finite-horizon constrained optimization problem obtained from the MPC method, and the current state is used as an initial state [23]. A feature of MPC-based approaches is that they can take into account various inequality constraints, and thus are able to enhance insensitivity to parameter variation and external disturbances [24]. In addition, for mobile robot, constraints for velocities and control inputs can be handled at the same time. One of the important issue for MPC implementation is the efficiency and effectiveness for real-time optimization. The reliability of any MPC approach is determined by the computational efficiency. In the literature, a number of approaches have been developed for the aim of reducing the computational burden of nonlinear MPC. In [12], robust model-based predictive control (RMPC) was investigated for the problem of missile interception. In [13], an adaptive neural predictive nonlinear controller for the nonholonomic mobile robot was proposed to track the trajectory. The MPC method can be implemented in [12] and [13] straightly because there exist smooth control method for these two system, however, the nonholonomic robot system cannot implement the MPC method straightly owing to the Brockett's theorem. In this work, through combing the theory of perturbed linear systems, the nonholonomic robot system is transform into two chained subsystems and a perturbation is added as an incentive term to maintain the controllability, after that, the MPC method can be finally applied to stabilize the transformed chained systems.

In this paper, by exploiting the special structure of the dynamics of the developed mobile robot, the nonholonomic kinematic subsystem is transformed into a skew-symmetric form, and then combine an exponential decaying term to solve the uncontrollable problem caused by the vanishing control input u_1. A model predictive control (MPC) strategy is thereafter developed for controlling the systems. The the optimization of MPC can be formulated as a convex nonlinear minimization problem. Then, a LVI-PDNN method can be used to solve this convex optimization problem over a finite receding horizon. Another issue of the MPC controller is the high computation cost. The applied neural networks can make the cost function of MPC converge to the exact optimal values of the formulated constrained QP. Extensive experiments have been performed to illustrate that MPC scheme has an effective performance on several real mobile robot systems.

II. Mobile Robot Control System

A. Kinematics and driving constraints

The general kinematic motion equations of the mobile robot subject to nonintegrable constraint of the mobile robot can be described as below:

$$N(p)\dot{p} = \dot{x}\sin\theta - \dot{y}\cos\theta = 0 \tag{1}$$

resulting from the assumption that the robot cannot slip in a lateral direction. In (1), $N(p) = [\sin\theta, -\cos\theta, 0]$ and it is defined over the generalized coordinates $p(t) = [x(t), y(t), \theta(t)]^T$. By expressing all the achievable velocities of the mobile robot as a linear combination of the vector fields that span the null space of the matrix $N(p)$, we can get the first-order kinematics model which can be described as following:

$$\dot{p}(t) = \begin{bmatrix} \dot{x}(t) \\ \dot{y}(t) \\ \dot{\theta}(t) \end{bmatrix} = \begin{bmatrix} \cos\theta(t) & 0 \\ \sin\theta(t) & 0 \\ 0 & 1 \end{bmatrix} \begin{bmatrix} v(t) \\ \omega(t) \end{bmatrix} \tag{2}$$

where $\omega(t)$ represents the angular velocity and $v(t)$ represents the longitudinal velocity of the mobile robot.

B. Chained System

For system (2), we can introduce a new coordinate as $x_1 = \theta$, $\xi_1 = x\sin\theta - y\cos\theta$, $\xi_2 = x\cos\theta + y\sin\theta$, $u_1 = \omega$, $u_2 = v - \omega\xi_1$ [36], then we have the chained form system as

$$\dot{x}_1 = u_1,\ \dot{\xi}_1 = \xi_2 u_1,\ \dot{\xi}_2 = u_2 \tag{3}$$

Let us transform (3) into two subsystems

$$\dot{x}_1 = u_1 \tag{4}$$

$$\dot{\xi} = \begin{bmatrix} \xi_2 u_1 \\ u_2 \end{bmatrix} \tag{5}$$

where $\xi = [\xi_1, \xi_2]$ is the state of the system (5). The two subsystems (4) and (5) can be then rewritten as following single input form:

$$\dot{x}_1 = f_1(x_1) + g_1(x_1)u_1 \tag{6}$$

$$\dot{\xi} = f_2(\xi, u_1) + g_2(\xi)u_2 \tag{7}$$

where $f_1(x_1) = 0$, $g_1(x_1) = 1$, $f_2(\xi, u_1) \in R^2$ and $g_2(\xi) \in R^2$ are defined below: $f_2(\xi, u_1) = [u_1\xi_2, 0]^T$, $g_2(\xi) = [0, 1]^T$.

It is noted that the second subsystem (7), the linear controllability is not guaranteed around its origin. In addition, the feedback control of continuous state is not able to stabilize this system because of its nonlinear characteristics. When the systems initial state is on the singular manifold, i.e., the initial state $x_1(0) = 0$, the corresponding control input $u_1(0) = 0$ will make the the states of subsystem (7) uncontrollable. To prevent the system from being uncontrollable, during the control process, we should make $x_1(t)$ out of singular manifold. For this purpose, inspired by [17] and [18], in this work we add an exponential decaying term into the control input such that it becomes

$$u_1 = u_1^* + \lambda e^{-\alpha t}. \tag{8}$$

The notation α is a positive constant and λ is a nonzero constant that represents the weight of the disturbance term. u_1^* is the optimal input for (6), the design of it will be described in Section III and the proving of convergence and the property for controlling (6) will be shown in Section V. The exponential decaying term $\lambda e^{-\alpha t}$ is global convergence and has boundness, so the properties of convergence and the boundness of combination u_1 are mainly dominated by u_1^*. Obviously, as the time past, u_1 will gradually converge to u_1^*. Noted that the additional exponential decaying term is supposed to postpone the input u_1 decaying to 0 so that the subsystem (7) keeps its controllability until subsystem (6) had approached to the original point

For controlling the robot system, the input u_1 can be applied as input $\omega = u_1$, while the u_2 requires a inverse transformation to get v:

$$v = u_2 + u_1\xi_1. \tag{9}$$

III. Robust Model Predictive Control Scheme

A. The Formulation of Model Predictive Control

A general discrete-time nonlinear system can be represented as following:

$$\mathbf{x}(k+1) = f(\mathbf{x}(k)) + g(\mathbf{x}(k))u(k) \tag{10}$$

subject to constraints specified $\mathbf{x}(k) \in \mathcal{X}$, $k = 1, 2, \ldots, N$; $u(k) \in \mathcal{U}$, $k = 1, 2, \ldots, N_u$, where m =1 or 2, $\mathbf{x} \in R^m$ represents the state vector; $u \in R$ represents the input vector; $f(\cdot) \in R^m$ and $g(\cdot) \in R^m$ represent assumed continuous nonlinear functions with $f(0) = 0$. The compact sets $\mathcal{X} \in R^m$ and $\mathcal{U} \in R$ comprise the origin in their interiors; N_u represents the control horizon and N represents the prediction horizon. And we have $1 \leq N$ and $0 \leq N_u \leq N$.

The control objective for the system (10) is to stabilize the state to the origin point using the MPC method, so we can define the following cost function as

$$\Gamma(k) = \sum_{j=1}^{N} ||\mathbf{x}^T(k+j|k)||_Q^2 + \sum_{j=0}^{N_u-1} ||\Delta u^T(k+j|k)||_R^2. \tag{11}$$

In the quadratic form, Q and R represent appropriate weighting matrices; $\Delta u(k+j|k)$ represents the increment of system input, i.e., $\Delta u(k+j|k) = u(k+j|k) - u(k-1+j|k)$ and the $\mathbf{x}(k+j|k)$ represents the predicted future horizon state; $\|\cdot\|$ denotes the Euclidean norm of the corresponding vector. From a theoretical point of view, a finite prediction and control horizon, i.e., N, N_u which are large enough in stage cost P is desirable as it will guarantee stability. For the system (10), we can acquire a quadratic problem for optimization by using the cost function (11), and its optimal solution can be obtained efficiently and reliably.

B. The Constraints of Mobile Robot System

We perform discretilization by using Taylor expansion, and ignoring the higher order term as

$$x(k+1) = x(k) + \dot{x}(k)T \tag{12}$$

where T represents the sampling period. Similar as (12), the two subsystems (6) and (7) can be rewritten as two nonlinear affine systems as

$$\begin{aligned} x_1(k+1) &= x_1(k) + Tu_1(k) \\ &= f_1(x_1(k)) + g_1(x_1(k))u_1(k) \end{aligned} \tag{13}$$

and

$$\begin{aligned} \xi(k+1) &= \begin{bmatrix} \xi_1 \\ \xi_2 \end{bmatrix} + \begin{bmatrix} Tu_1\xi_2 \\ -Tu_1\xi_1 \end{bmatrix} + \begin{bmatrix} 0 \\ T \end{bmatrix} u_2(k) \\ &= f_2(\xi(k), u_1(k)) + g(\xi(k))u_2(k) \end{aligned} \tag{14}$$

subject to constraints

$$u_{1min} \leqslant u_1(k) \leqslant u_{1max} \tag{15}$$
$$u_{2min} \leqslant u_2(k) \leqslant u_{2max} \tag{16}$$
$$\Delta u_{1min} \leqslant \Delta u_1(k) \leqslant \Delta u_{1max} \tag{17}$$
$$\Delta u_{2min} \leqslant \Delta u_2(k) \leqslant \Delta u_{2max} \tag{18}$$
$$x_{1min} \leqslant x_1(k) \leqslant x_{1max} \tag{19}$$
$$\xi_{min} \leqslant \xi(k) \leqslant \xi_{max} \tag{20}$$

where T represents the sampling period, $\xi = [\xi_1, \xi_2]^T$ is the state vector of the subsystem (14).

Remark 3.1: The inequalities for vectors used in (20) are element-wise, e.g., $\xi_{jmin} \leqslant \xi_j(k) \leqslant \xi_{jmax}$, for $j = 1, 2$, where ξ_j represents the jth element in the vector.

For $i = 1, 2$, the following vectors are defined:

$$\bar{x}_1(k) = [x_1(k+1|k), \ldots, x_1(k+N|k)]^T \in R^N \tag{21}$$
$$\bar{\xi}(k) = [\xi(k+1|k), \ldots, \xi(k+N|k)]^T \in R^{2N} \tag{22}$$
$$\bar{u}_i(k) = [u_i(k|k), \ldots, u_i(k+N_u-1|k)]^T \in R^{N_u} \tag{23}$$
$$\Delta\bar{u}_i(k) = [\Delta u_i(k|k), \ldots, \Delta u_i(k+N_u-1|k)]^T \in R^{N_u}. \tag{24}$$

Let us define a vector $[\bar{\mathbf{x}}_1, \bar{\mathbf{x}}_2] = [\bar{x}_1, \bar{\xi}]$. According to (13) and (14), for $i = 1, 2$, we can predict the future state $\mathbf{x}_i(k+j|k), j = 1, 2, \ldots, N$ at sampling instant k by applying the optimal input obtained at the previous instant, i.e., $u_i(k+j|k-1), j = 1, 2, \ldots, N_u$ as follow:

$$\begin{aligned} &\mathbf{x}_i(k+1|k) = f_i(\mathbf{x}_i(k|k-1)) + g_i(\mathbf{x}_i(k|k-1)) \\ &\times(u_i(k-1) + \Delta u_i(k|k)) \\ &\mathbf{x}_i(k+2|k) = f_i(\mathbf{x}_i(k+1|k-1)) + g_i(\mathbf{x}_i(k+1|k-1)) \\ &\times(u_i(k-1) + \Delta u_i(k|k) + \Delta u_i(k+1|k)) \\ &\quad\vdots \\ &\mathbf{x}_i(k+N|k) = f_i(\mathbf{x}_i(k+N|k-1)) \\ &+g_i(\mathbf{x}_i(k+N-1|k-1))(u_i(k-1) + \Delta u_i(k|k) \\ &+\ldots + \Delta u_i(k+N_u-1|k)) \end{aligned} \tag{25}$$

where $u_i(k-1)$ represents the applied control input at the previous instant, $\Delta u_i(k+j|k)$ represents the optimal input increment at the future time instance $k+j$, which can be obtained by solving the optimization problem at the current time instance k, $x_i(k+j|k)$ represents the predicted state at future time instance $k+j$ which can be predicted at the current time instance k by using the input $u_i(k+j|k) = \Delta u_i(k+j|k) + \ldots + \Delta u_i(k|k) + u_i(k-1)$.

Then, for $i = 1, 2$, the predicted output of two subsystems can be expressed as following:

$$\bar{\mathbf{x}}_i(k) = G_i\Delta\bar{u}_i(k) + \tilde{f}_i + \tilde{g}_i \tag{26}$$

where $G_i =$

$$\begin{bmatrix} g_i(\mathbf{x}_i(k|k-1)) & \ldots & 0 \\ g_i(\mathbf{x}_i(k+1|k-1)) & \ldots & 0 \\ \vdots & \ddots & \vdots \\ g_i(\mathbf{x}_i(k+N-1)|k-1)) & \ldots & g_i(\mathbf{x}_i(k+N-1)|k-1)) \end{bmatrix},$$

$\tilde{f}_i = [f_i(\mathbf{x}_i(k|k-1)), f_i(\mathbf{x}_i(k+1|k-1)), \ldots, f_i(\mathbf{x}_i(k+N-1|k-1))]^T$, $\tilde{g}_i = [g_i(\mathbf{x}_i(k|k-1))u_i(k-1), g_i(\mathbf{x}_i(k+1|k-1))u_i(k-1), \ldots, g_i(\mathbf{x}_i(k+N-1|k-1))u_i(k-1)]^T$. Hence, the original optimization objective (11) subject to constraints (15)–(20) can be rewritten as

$$\min \ \ \|G_i\Delta\bar{u}_i(k)+\tilde{f}_i+\tilde{g}_i\|_Q^2+\|\Delta\bar{u}_i(k)\|_R^2 \tag{27}$$

subject to $\Delta\bar{u}_{min}\leqslant\Delta\bar{u}(k)\leqslant\Delta\bar{u}_{max}$, $\bar{u}_{min}\leqslant\bar{u}_i(k-1)\leqslant\bar{u}_{max}$, $\bar{u}_{min}\leqslant\bar{u}_i(k-1)+\tilde{I}\Delta\bar{u}_i(k)\leqslant\bar{u}_{max}$, $\bar{\mathbf{x}}_{imin}\leqslant\tilde{f}_i+\tilde{g}_i+G_i\Delta\bar{u}_i(k)\leqslant\bar{\mathbf{x}}_{imax}$, where $\tilde{I}=\begin{bmatrix} I & 0 & \cdots & 0\\ I & I & \cdots & 0\\ \vdots & \vdots & \ddots & \vdots\\ I & I & \cdots & I\end{bmatrix}\in R^{N_u\times N_u}$.

Then the optimization objective (27) with disturbance can be rewritten as QP problems. Let $m=1$ or 2 as the dimension parameter for the ith subsystem where $i=1,2$. We have

$$\min \ \ \frac{1}{2}\Delta\bar{u}_i(k)^TW_{1i}\Delta\bar{u}_i(k)+c_{1i}^T\Delta\bar{u}_i(k) \tag{28}$$

subject to $E_{1i}\Delta\bar{u}_i\leqslant b_{1i}$, $\Delta\bar{u}_{min}\leqslant\Delta\bar{u}_i\leqslant\Delta\bar{u}_{max}$, where the coefficients are $W_{1i}=2G_i^TQG_i\in R^{N_u\times N_u}$, $c_{1i}=2G^TQ(\tilde{g}+\tilde{f})\in R^{N_u}$, $E_{1i}=\begin{bmatrix}-\tilde{I}\\ \tilde{I}\\ -G_i\\ G_i\end{bmatrix}\in R^{(2N_u+2mN)\times N_u}$, $b_{1i}=[-\bar{u}_{min}+\bar{u}_i(k-1),\bar{u}_{max}+\bar{u}_i(k-1),-\bar{\mathbf{x}}_{imin}+\tilde{f}_i+\tilde{g}_i,\bar{\mathbf{x}}_{imax}-\tilde{f}_i-\tilde{g}_i]^T\in R^{2N_u+2mN}$.

C. Robust MPC Formulation

It is always affected by disturbances which may be caused by various dynamic conditions, which are impossible to measure. Consider (13) and (14) with disturbances as

$$x_1(k+1)=f_1(x(k))+g_1(x_1(k))u_1(k)+d_1(k) \tag{29}$$
$$\xi(k+1)=f_2(\xi(k),u_1(k))+g(\xi(k))u_2(k)+d_2(k) \tag{30}$$

subject to constraints

$$u_{1min}\leqslant u_1(k)\leqslant u_{1max} \tag{31}$$
$$u_{2min}\leqslant u_2(k)\leqslant u_{2max} \tag{32}$$
$$\Delta u_{1min}\leqslant\Delta u_1(k)\leqslant\Delta u_{1max} \tag{33}$$
$$\Delta u_{2min}\leqslant\Delta u_2(k)\leqslant\Delta u_{2max} \tag{34}$$
$$x_{1min}\leqslant x_1(k)\leqslant x_{1max} \tag{35}$$
$$\xi_{min}\leqslant\xi(k)\leqslant\xi_{max} \tag{36}$$
$$d_{1min}\leqslant d_1(k)\leqslant d_{1max} \tag{37}$$
$$d_{2min}\leqslant d_2(k)\leqslant d_{2max} \tag{38}$$

where $d_1(k)\in R$ and $d_2(k)\in R^2$ are two bounded additive disturbances of the above subsystems.

Let us introduce the following vectors:

$$\bar{d}_1(k)=[d_1(k+1|k),\ldots,d_1(k+N|k)]^T\in R^N \tag{39}$$
$$\bar{d}_2(k)=[d_2(k+1|k),\ldots,d_2(k+N|k)]^T\in R^{2N}. \tag{40}$$

Similar as the previous definition of the parameters, for $i=1,2$, the predicted output of two subsystems can be expressed as following:

$$\bar{\mathbf{x}}_i(k)=G_i\Delta\bar{u}_i(k)+\tilde{f}_i+\tilde{g}_i+\bar{d}_i(k). \tag{41}$$

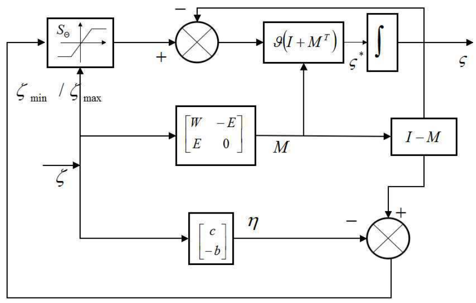

Fig. 1. Architecture of primal-dual neural network in (50).

Hence, the original optimization objective (11) subject to constraints (31)–(38) can be rewritten as

$$\min \ \ \|G_i\Delta\bar{u}_i(k)+\tilde{f}_i+\tilde{g}_i+\bar{d}_i(k)\|_Q^2+\|\Delta\bar{u}_i(k)\|_R^2 \tag{42}$$

subject to $\Delta\bar{u}_{min}\leqslant\Delta\bar{u}(k)\leqslant\Delta\bar{u}_{max}$, $\bar{u}_{min}\leqslant\bar{u}_i(k-1)\leqslant\bar{u}_{max}$, $\bar{u}_{min}\leqslant\bar{u}_i(k-1)+\tilde{I}\Delta\bar{u}_i(k)\leqslant\bar{u}_{max}$, $\bar{\mathbf{x}}_{imin}\leqslant\tilde{f}_i+\tilde{g}_i+G_i\Delta\bar{u}_i(k)\leqslant\bar{\mathbf{x}}_{imax}$, $\bar{d}_{min}\leqslant\bar{d}_i(k)\leqslant\bar{d}_{max}$.

Then, the optimization objective (27) with disturbance can be rewritten as QP problems. Let integer $m=1$ or 2 be the dimension parameter for the ith subsystem where $i=1,2$. We have

$$\min \ \ \begin{bmatrix}\Delta\bar{u}_i(k)\\ \bar{d}_i(k)\end{bmatrix}^T W_i\begin{bmatrix}\Delta\bar{u}_i(k)\\ \bar{d}_i(k)\end{bmatrix}+c_i^T\begin{bmatrix}\Delta\bar{u}_i(k)\\ \bar{d}_i(k)\end{bmatrix} \tag{43}$$

subject to

$$E_i\begin{bmatrix}\Delta\bar{u}_i(k)\\ \bar{d}_i(k)\end{bmatrix}\leqslant b_i \tag{44}$$

where $W_i=\begin{bmatrix}G_i^TQG_i+R & G_i^TQ\\ QG_i & Q\end{bmatrix}\in R^{(N_u+mN)\times(N_u+mN)}$, $c_i=[2G^TQ(\tilde{g}+\tilde{f}),2Q(\tilde{g}+\tilde{f})]\in R^{(N_u+mN)}$, $E_i=\begin{bmatrix}E_{1i} & 0\\ I & 0\\ 0 & I\\ -I & 0\\ 0 & -I\end{bmatrix}\in R^{(4N_u+4mN)\times(N_u+mN)}$, $b_i=[b_{1i},\Delta\bar{u}_{max},\bar{d}_{max},-\Delta\bar{u}_{min},-\bar{d}_{min}]^T\in R^{4N_u+4mN}$, E_{1i} and b_{1i} are defined in Subsection III-B. Let $\zeta_i=[\Delta\bar{u}_i(k),\bar{d}_i(k)]^T$, then (43), (44) can be rewritten as follows:

$$\min \ \ \zeta_i^TW_i\zeta_i+c_i^T\zeta_i \tag{45}$$

subject to

$$E_i\zeta_i\leqslant b_i. \tag{46}$$

IV. Primal-dual Neural Network Optimization

For the MPC, a unified quadratic programming (QP) formulation (28) and (43)is proposed, so we need to seek an online approach to solve the QP problem efficiently. For constraints (15)–(20) and (31)–(38), $y\in R^{N_M}$ is defined as the corresponding dual decision vector, where $N_M=4N_u+4mN$

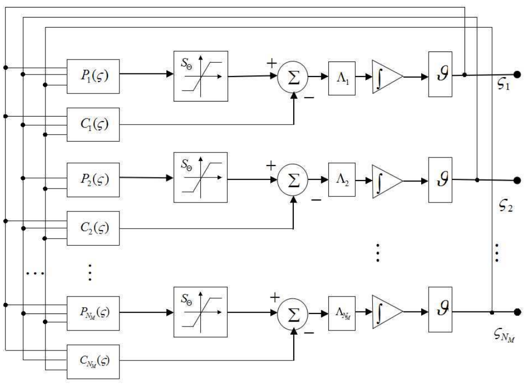

Fig. 2. Block diagram of primal-dual dynamical system.

or $N_M = 2N_u + 2mN$ depends on whether considering disturbance and $m = 1$ or $m = 2$. Hence, we define ς as the primal-dual decision vector and the upper/lower bounds of it are $\varsigma^{\pm}$. These two terms are represented as following respectively:

$$\varsigma := \begin{bmatrix} \zeta \\ y \end{bmatrix}, \quad \varsigma^{+} := \begin{bmatrix} \zeta_{max} \\ +y^{+} \end{bmatrix}, \quad \varsigma^{-} := \begin{bmatrix} \zeta_{min} \\ -y^{-} \end{bmatrix} \in R^{N_M} \tag{47}$$

where for any index i, the elements $y_i^{+} \gg 0$ in y^{+} denotes $+\infty$. Thus, the convex set Θ can be presented as $\Theta = \{\varsigma^{-} \leqslant \varsigma \leqslant \varsigma^{+}\}$, where ς is primal-dual decision vector. Let the coefficient matrix $M \in R^{N_M \times N_M}$ and vector $\eta \in R^{N_M}$ being

$$M = \begin{bmatrix} W & -E^T \\ E & 0 \end{bmatrix} \quad \eta = \begin{bmatrix} c \\ -b \end{bmatrix}. \tag{48}$$

Then, we are ready to prove the following theorem for the optimization of (28).

Theorem 4.1: [27](LVI Formulation) Quadratic programming (43)–(44) is to find a vector $\varsigma^* \in \Theta = \{\varsigma | \varsigma^{-} \leqslant \varsigma \leqslant \varsigma^{+}\}$ that satisfies the following linear variational inequalities:

$$(\varsigma - \varsigma^*)^T (M\varsigma^* + \eta) \geqslant 0, \quad \forall \varsigma \in \Theta \tag{49}$$

where coefficients M, η, and $\varsigma^{\pm}$ are defined in (47) and (48), respectively.

According to [27], the linear variational inequality (49) can be transformed into piecewise linear equation as following system

$$S_\Theta\left(\varsigma - (M\varsigma + \eta)\right) - \varsigma = 0 \tag{50}$$

where $S_\Theta(\cdot)$ represents the projection operator onto Θ and defined as $S_\Theta(\varsigma) = [S_\Theta(\varsigma_1), \cdots, S_\Theta(\varsigma_{N_M})]^T$ with

$$S_\Theta(\varsigma_i) = \begin{cases} \varsigma^{-} & \text{if } \varsigma_i < \varsigma^{-}, \\ \varsigma_i & \text{if } \varsigma^{-} \leqslant \varsigma_i \leqslant \varsigma^{+}, \forall i \in R^{N_M}. \\ \varsigma^{+} & \text{if } \varsigma_i > \varsigma^{+}, \end{cases}$$

To solve the linear projection equation (50), we can develop the following modified dynamic system to solve (50)

$$\dot{\varsigma} = \vartheta (I + M^T)\{S_\Theta\left(\varsigma - (M\varsigma + \eta)\right) - \varsigma\}, \tag{51}$$

where ϑ represents a strictly-positive design parameter, by adjusting which the convergence rate of the system can be tuned. Let $\Lambda = I + M^T$, $P(\varsigma) = \varsigma - (M\varsigma + \eta)$, and $C(\varsigma) = \varsigma$, we can simplify (51) as

$$\dot{\varsigma} = \vartheta \Lambda (S_\Theta\left(P(\varsigma)\right) - C(\varsigma)). \tag{52}$$

Remark 4.1: The neural network structure is shown in Figure 1, where Λ_i represents the ith row of the scaling matrix Λ. When the dimensions of input ς is N_M, the neural network consists of N_M integrators, $4N_M$ summers, N_M processors of projection operator $S_\Theta(\cdot)$ and N_M processors of vector-valued function $P(\varsigma)$ and $C(\varsigma)$. Figure 2 describes the block diagram of primal-dual dynamical system (51). In the dynamic control process, $\zeta = [\Delta\bar{u}, \bar{d}(k)]^T$ is first fed into the system after constituting the coefficient matrices and vectors like W, b, E, ζ_{min}, and ζ_{max}. We can obtain the outputs the signal $\varsigma(t)$ from primal-dual dynamic system, and the first N_u elements of it are $\Delta\bar{u}$.

Fig. 3 shows the control structure of the proposed MPC approach. Therefore, the summarization of MPC for the chained non-holonomic systems (2) based on this PDNN method can be described as follows:

1) Let $k = 1$, and choose period T, control horizon N_u, prediction horizon N, coefficients ϑ, λ and α and weight matrices R and Q.
2) Partition the robot systems (2) into two subsystems (6) and (7). Considering the disturbance $d(k)$, we can formulate QP form (28). For $i = 1, 2$, we get W_i, c_i, E_i, b_i, and set the upper/lower bounds ς^{-}, ς^{+}.
3) Use the PDNN method to solve (43) of the first subsystem (6) by solving the differential equation (50), and obtain its optimal control increment vector sequence $\Delta\bar{u}_1(k)$. Only the first term of $\Delta\bar{u}_1(k)$ is used to calculate $u_1^*(k+1)$, then (8) is used to obtain the $\omega(k+1) = u_1(k+1)$.
4) Similar to step 3), calculate the control input $v(k+1) = u_2(k+1) + u_1(k+1)\xi_1(k)$ from (9).
5) Use the $\omega(k+1)$ and $v(k+1)$ as the control inputs during current sampling period for the wheeled robot. According to the current position, calculate the position $(x(k+1), y(k+1))$ and the heading direction $\theta(k+1)$ of the mobile robot (2).
6) After the transformation, we can obtain the $x_1(k+1)$ and $[\xi_1(k+1), \xi_2(k+1)]$ for the calculation of next period.
7) If the robot does not reach the origin, it goes to step 2) and set $k = k + 1$. Otherwise, the robot will arrive the goal.

Remark 4.2: PDNN does not depend on penalty or analog parameters, matrix inverses, or high-order nonlinear terms, only with simple vector or matrix augmentation and operation. Consequently, the architecture of the PDNN to be implemented on analog circuits could be much simpler than those of the existing recurrent neural networks [30], [31]. Consider the time-varying nature of QP (43)–(44). Define $N_M = 5N_u + 5mN$, the applied PDNN method in this work contains N_M integrators, $4N_M$ summers, $2N_M^2$ multiplications and N_M limiter-operations per iteration, so the PDNN has $O(6(5N_u{+}5mN){+}2(5N_u{+}5mN))^2$ operations. To solve the QP optimization, we use a traditional gradient descent based SQP methods to get the optimal solution, while this method

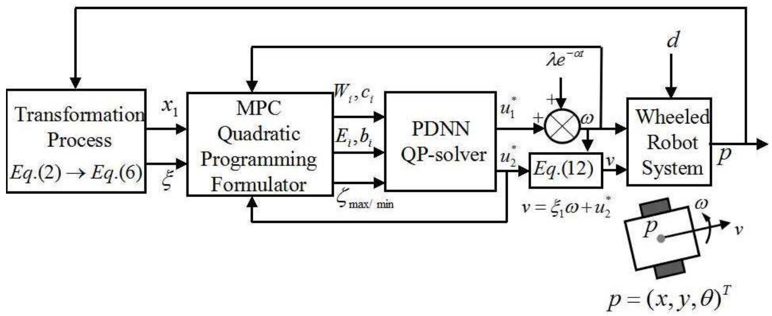

Fig. 3. The control structure of the proposed MPC approach.

require repeatedly calculating the Hessian matrix to solve a quadratic program, and has high computational complexity [32], [33]. For example, the MATLAB optimization routines "QUADPROG" or "LINPROG" function. On the other hand, the traditional QP solution needs $O((mN)^4 + mN + N_u^2 \times (5N_u + 5mN) + (6N_u + 5mN)^3)$ operations for its online computation requirement and obviously is not appropriate for the mobile robot systems, due to inefficient numerical algorithm. It is clear that the proposed PDNN approach can reduce the computation cost. For solving the QP problem (43)–(44) in this work, the computational time of the traditional SQP approach costs about 0.3 s, while the PDNN approach only takes 0.038s (Note that the experiments were run on a PC with a CPU of Inter(R) Pentium(R) E5700 @ 3.00 GHz, 2GB memory), which is smaller than the sampling time 0.1s. Therefore, PDNN method can be implemented in real-time for our experiments.

V. Stability Analysis

In each sampling period, we solve the PDNN dynamic system (51) to obtain the optimal input for the system, so for each period, the convergence of (51) should be considered. By ignoring the disturbance term, we can rewrite the above nonlinear discrete-time system (10) as follows:

$$\begin{aligned} x(k+1) &= f(x(k)) + g(x(k))u(k)) \\ &= \varphi(x(k), u(k-1), \Delta u(k)) \end{aligned} \tag{53}$$

which is subject to constraints specified below

$$x(k) \in \mathcal{X},\ k = 1, 2, \dots, N \tag{54}$$
$$u(k-1) \in \mathcal{U},\ k = 1, 2, \dots, N_u - 1 \tag{55}$$
$$\Delta u(k) \in \Delta\mathcal{U},\ k = 1, 2, \dots, N_u - 1 \tag{56}$$

where $\Delta u(k) = u(k) - u(k-1)$. The system (53) has properties specified below:

Property 5.1: $\varphi(\cdot) \in R^m$ is continuous, and $\varphi(0,0,0) = 0$, whereas $(0,0,0)$ is the equilibrium point of the system.

Property 5.2: The $\mathcal{U}, \Delta\mathcal{U} \in R$ and $\mathcal{X}$ are compact sets, inside the set $\mathcal{X} \times \mathcal{U} \times \Delta\mathcal{U}$ contains the origin point $(0,0,0)$. Define that $\bar{x}(k) = [x(k+1|k), \dots, x(k+N|k)]^T \in R^N$, $\bar{u}(k) = [u(k|k), \dots, u(k+N_u-1|k)]^T \in R^{N_u}$, $\Delta\bar{u}(k) = [\Delta u(k|k), \dots, \Delta u(k+N_u-1|k)]^T \in R^{N_u}$. We aim to solve the following optimization problem:

$$\begin{aligned} &\min \Gamma(K) = \min \Gamma(x(k), \Delta\bar{u}(k)) \\ &= \min_{\Delta\bar{u}(k)} ||\bar{x}^T(k+j|k)||_Q^2 + ||\Delta\bar{u}^T(k+j|k)||_R^2 \end{aligned} \tag{57}$$

We can choose N and N_u to be large enough. If there exists control increment sequence $\Delta\bar{u}(k)$ for arbitrary $j = 1, 2, \dots, N$ such that the constraints (54)–(56) can be satisfied, then for the optimal problem, $\Delta\bar{u}(k)$ is its feasible solution. Assume that at the time instant k, the optimal solutions $\Delta\bar{u}^*(k)$ is $\Delta\bar{u}^*(k) = [\Delta u^*(k|k), \dots, \Delta u^*(k+N_u-1|k)]^T \in R^{N_u}$, and states $\bar{x}^*(k) = [x^*(k+1|k), \dots, x^*(k+N|k)]^T \in R^N$ are the optimal states trajectory so that the control increment at the time k is $\Delta u(k) := \Delta u^*(k|k)$.

Assume that there exist feasible solutions for the the optimal problem and the function of optimal value is defined as:

$$\mathbb{E}(x) = \min_{\Delta\bar{u}(k)} \Gamma(x(k), \Delta\bar{u}(k)). \tag{58}$$

Then we have

Theorem 5.1: The discrete-time systems of finite prediction MPC optimal function have the following properties:

- (i) $\mathbb{E}(0) = 0$ and for arbitrary $x \neq 0$, $\mathbb{E}(x) > 0$ is continuous at $x = 0$;
- (ii) Consider every sampling periodic time, no matter what initial state starts, the state vector $\varsigma(t)$ (51) can exponentially converges to an equilibrium point ς^* and satisfy $\|\varsigma - S_\Theta(\varsigma - (M\varsigma + \eta))\|^2 \geqslant \rho\|\varsigma - \varsigma^*\|^2$ with a constant $\rho > 0$.
- (iii) $\mathbb{E}(x)$ is monotone decreasing along the trajectory of system.

Proof: Considering the projection inequality $(\varpi - S_\Theta(\omega))^T(\omega - S_\Theta(\omega)) \leqslant 0$ for all $\omega \in R^{N_M}$ and $\varpi \in \Theta$ [34], we have the following inequality in every sampling period $(\varsigma^* - S_\Theta(\varsigma - (M\varsigma + \eta)))^T(\varsigma - (M\varsigma + \eta) - S_\Theta(\varsigma - (M\varsigma + \eta))) \leqslant 0$. Then, considering the projection-equation reformulation of the linear variational inequality (50), we have $(\varsigma^* - S_\Theta(\varsigma - (M\varsigma + \eta)))^T(-\eta + M\varsigma^*) \leqslant 0$. Combining both yields

$$\begin{gathered} (-\varsigma^* + S_\Theta(\varsigma - (M\varsigma + \eta)))^T \times \\ (M(\varsigma - \varsigma^*) - \varsigma + S_\Theta(\varsigma - (M\varsigma + \eta))) \leqslant 0 \end{gathered} \tag{59}$$

$$\begin{gathered} (\varsigma - \varsigma^* - \varsigma + S_\Theta(\varsigma - (M\varsigma + \eta)))^T \times \\ (M(\varsigma - \varsigma^*) - \varsigma + S_\Theta(\varsigma - (M\varsigma + \eta))) \leqslant 0 \end{gathered} \tag{60}$$

Then, from (60), we can further obtain

$$\begin{aligned} & (\varsigma-\varsigma^*)^T(I+M^T)(S_\Theta(\varsigma-(M\varsigma+\eta))-\varsigma) \\ \leqslant \quad & -(\varsigma-\varsigma^*)^T M(\varsigma-\varsigma^*)-\|S_\Theta(\varsigma-(M\varsigma+\eta))-\varsigma\|^2 \quad (61) \end{aligned}$$

Consider that M is positive semi-definite (not necessarily symmetric), i.e.,

$$\varsigma^T M\varsigma=\varsigma^T\frac{M+M^T}{2}\varsigma=\varsigma^T\begin{bmatrix} W & 0 \\ 0 & 0\end{bmatrix}\varsigma\geqslant 0. \quad (62)$$

Then, we have

$$\begin{aligned} & (\varsigma-\varsigma^*)(I+M^T)(S_\Theta(\varsigma-(M\varsigma+\eta))-\varsigma) \\ \leqslant & -\|\varsigma-\varsigma^*\|_M^2-\|S_\Theta(\varsigma-(M\varsigma+\eta))-\varsigma\|^2\leqslant 0. \end{aligned}$$

Define a Lyapunov function $\mathbb{K}(\varsigma)=\|\varsigma-\varsigma^*\|^2$. Along the primal-dual neural network trajectory (51), its time derivative is

$$\begin{aligned} \frac{d\mathbb{K}(\varsigma)}{dt} &= (\frac{\partial\mathbb{K}(\varsigma)}{\partial\varsigma})^T\frac{d\varsigma}{dt} \\ &= \vartheta(\varsigma-\varsigma^*)^T(I+M^T)(S_\Theta(\varsigma-(M\varsigma+\eta))-\varsigma) \\ &\leqslant -\vartheta\|\varsigma-\varsigma^*\|_M^2-\vartheta\|S_\Theta(\varsigma-(M\varsigma+\eta))-\varsigma\|^2 \\ &\leqslant 0. \end{aligned} \quad (63)$$

According to Lyapunov theory, the state $\varsigma(t)$ of the system is stable and globally convergent to an equilibrium ς^*, because that $\dot{\mathbb{K}}=0$ when $\dot{\varsigma}=0$ and $\varsigma=\varsigma^*$. The work [35] and (50) elucidate that for the linear variational inequality problem (49), ς^* is a solution, and the optimal solution Δu^* to quadratic programming is the first N_u elements of ς^*. Regarding the exponential convergence, from (63) and the (ii) of Theorem 5.1, we can review $\mathbb{K}(\varsigma)$ and $\dot{\mathbb{K}}(\varsigma)$ and get that:

$$\begin{aligned} \frac{d\mathbb{K}(\varsigma)}{dt} &\leqslant -\vartheta\|\varsigma-\varsigma^*\|_M^2-\vartheta\|S_\Theta(\varsigma-(M\varsigma+\eta))-\varsigma\|^2 \\ &\leqslant -\vartheta\|\varsigma-\varsigma^*\|_M^2-\vartheta\rho\|\varsigma-\varsigma^*\|^2 \\ &= -\vartheta(\varsigma-\varsigma^*)^T(\rho I+M)(\varsigma-\varsigma^*) \\ &\leqslant -\phi\mathbb{K}(\varsigma) \end{aligned} \quad (64)$$

where $\phi=\vartheta\rho$ is the convergence rate. Thus, we have $\mathbb{K}(\varsigma)=C(e^{-\phi(t-t_0)}),\forall t\geqslant t_0$, so that $\|\varsigma-\varsigma^*\|=C(e^{-\frac{\phi(t-t_0)}{2}}),\forall t\geqslant t_0$, until now the exponential convergence property of this primal-dual network is established.

Assume that a time instant k, the finite horizon constraints optimal question has the feasible solutions

$$\Delta\bar{u}^*(k)=[\Delta u^*(k|k),\dots,\Delta u^*(k+N_u-1|k)]^T\in R^{N_u} \quad (65)$$

and then by using $u^*(k+j|k)=u(k-1)+\Delta u^*(k|k)+\ldots+\Delta u^*(k+j|k),\quad j=0,1,\dots,N_u-1$, we can get

$$\bar{u}^*(k)=[u^*(k|k),\dots,u^*(k+N_u-1|k)]^T\in R^{N_u} \quad (66)$$

satisfying the constraints (55).

Therefore, the output of sequence state is $\bar{x}^*(k)=[x^*(k+1|k),\dots,x^*(k+N|k)]^T\in R^N$, which satisfies the states constraints. For the system with additive disturbance, at the time instant $k+1$, the system's closed-loop states observations is

$$x(k+1)=\varphi(x(k),u(k-1),\Delta u^*(k|k)) \quad (67)$$

and its value is consistent with the predicted states at time instant $k+1$. We can choose the control input increment and control input sequence

$$\begin{aligned} &\Delta\bar{u}(k+1)=[\Delta u(k+1|k+1),\dots,\Delta u(k+N_u|k+1)] \\ &=[\Delta u^*(k+1|k),\dots,\Delta u^*(k+N_u|k)] \\ &\bar{u}(k+1)=[u(k+1|k+1),\dots,u(k+N_u|k+1)] \\ &=[u^*(k+1|k),\dots,u^*(k+N_u|k). \end{aligned} \quad (68)$$

which are the parameter of states sequence, $u^*(k+j+1|k)=u(k)+\Delta u^*(k+1|k)+\ldots+\Delta u^*(k+j+1|k),j=0,1,\dots,N_u-1$. The states sequence is $x(k+1+j|k+1)=x^*(k+1+j|k)$, $j=1,2,\dots,N$, which satisfies the states constraints. At the time instant $k+1$, we can calculate the objective function

$$\begin{aligned} \Gamma(K+1) &= \sum_{i=1}^{N}\|x^T(k+i+1|k+1)\|_Q^2 \\ &\quad+\sum_{j=0}^{Nu-1}\|\Delta u^T(k+j+1|k+1)\|_R^2 \\ &= \sum_{j=2}^{N}\|x^{*T}(k+j|k)\|_Q^2+\sum_{j=1}^{N_u-1}\|\Delta u^T(k+j|k)\|_R^2 \\ &= \sum_{j=1}^{N}\|x^{*T}(k+j|k)\|_Q^2+\sum_{j=0}^{N_u-1}\|\Delta u^T(k+j|k)\|_R^2- \\ &\quad \|x^T(k|k)\|_Q^2-\|\Delta u^T(k|k)\|_R^2 \\ &= \mathbb{E}(x(k))-\|x^T(k|k)\|_Q^2-\|\Delta u^T(k|k)\|_R^2. \end{aligned}$$

Obviously, $\Gamma(K+1)$ is bounded such that the selected control input sequence (68) at time instant $k+1$ is a feasible solution of the finite horizon constraints optimal question. According to (58), the optimal solution is not worse than the feasible solution and R is a symmetric positive definite matrix. Then, we have

$$\mathbb{E}(x(k+1))\leqslant\Gamma(K+1)\leqslant\mathbb{E}(x(k))-\|x^T(k)\|_Q^2. \quad (69)$$

Therefore, $\mathbb{E}(x)$ is monotone decreasing along the trajectory of system. ■

We can choose the optimal value function $\mathbb{E}(x(k))$ as one of the Lyapunov function of the system and according to (69), we have

$$\mathbb{E}(x(k+1))-\mathbb{E}(x(k))\leqslant-\lambda_{min}(Q)||x^T(k)||^2, \quad (70)$$

so the system is nominally asymptotically stable.

Remark 5.1: Note that the bounded disturbances $d_i(k)$ (with bounds d_{min} and d_{max}) have been considered in the optimization objective function (42), which is used to solve for the optimal solution by using RMPC method. When PDNN in (51) is applied to solve the QP problem (42), the disturbances $d_i(k)$ (the boundedness d_{min} and d_{max}) have been already considered. Thus, we obtain the optimal solution $\Delta\bar{u}^*(k)$ in the presence of the disturbances, so that robustness is ensured for the proposed optimal control.

Remark 5.2: In this work, we choose these parameters (λ, α and ϑ) based on the experience of designer accumulated from trial and error in simulation and experiment studies. In fact, there is no general criteria for the selection of control parameters for nonlinear control. The influence on the system behaviour can be evaluated by trial and error through the experimental tests or simulations.

VI. EXPERIMENTS

A. Robot Description and Control Architecture

In order to test the robustness of the developed control method on different dynamic loads, two mobile robots with different sizes and masses are employed in the experiments. The robots are shown in Fig. 4. The smaller guide robot has mass of about $85kg$ and has size of $120cm \times 60cm \times 55cm$ and we define it as Rob_1. The bigger one is defined as Rob_2, which has mass of about $121kg$ and size of $142cm \times 70cm \times 62cm$. Under the conditions of different sizes and weights, the control parameters of two robots are exactly same for robustness tests. Both Rob_1 and Rob_2 are equipped with two driving wheels with powerful motors as well as two passive wheels for balance purpose.The wheels of radius of $19.5cm$ are mounted on a chassis of length $45cm$. The $24V$ rated voltage motors drive the wheels with rated torque $72.1mNm/A$ at $5200rpm$. Two 2048 pulses/turn counting incremental encoders are equipped on each motor of the these robots to get the motion data. There is also a drive gear assembly equipped on each motor which reduces the speed by a factor of 85.33.

The two-level control structure of these two robots is shown in Fig.4. The VC++ written algorithms constitute the high-level control layer, and the reference motion generation is included in it. The algorithms runs on a host computer (Intel 2-core processor) with a sampling time of 100 ms. The host compute and Elmo driver communicates through using the CAN bus and the servo motor is controlled using the computed torque. The odometric is computed through the data measured from the encoder. The velocity commands from the high-level control layer will be executed by the lower level control layer. This layer consists of Elmo driver controller. The Elmo driver controller has three important task during the control 1) through the Kvaser, CAN device, communicate with the higher-level controller; 2) to generate the computed input torques; and 3) to obtain the counts data from encoder interrupt driven.

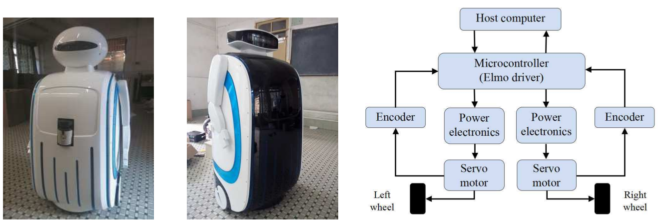

Rob_1 Rob_2 Control structure

Fig. 4. The guide wheeled mobile robots, they have same control structures and control parameters.

B. Control Command and Physical Constraints

For the wheeled mobile robot, we define ω_{max} and v_{max} as its maximum control inputs, then the current curvature $\kappa = \omega/v$ is preserved owing to the saturation of the command velocities [29], which can be performed as $\varrho = \max\{1, |\omega|/\omega_{max}, |v|/v_{max}\}$, where the actual command velocities ω_c and v_c represent as following

$$\begin{cases} \omega_c = \omega,\ v_c = v, & \text{if } \varrho = 1, \\ \omega_c = \omega_{max}\mathrm{sgn}(\omega),\ v_c = v/\varrho, & \text{if } \varrho = |\omega|/\omega_{max}, \\ \omega_c = \omega/\varrho,\ v_c = v_{max}\mathrm{sgn}(v), & \text{if } \varrho = |v|/v_{max}, \end{cases}$$

The wheeled mobile robot is controlled by the low-level control layer, so in each time instant k we need to transform $\omega(k)$ and $v(k)$ into robot's left-wheel velocity $v_L(k)$ and the right-wheel velocity $v_L(k)$, which can be represented as $v_L(k) = v(k) - \omega(k)L/2$, and $v_R(k) = v(k) + \omega(k)L/2$, where L is the diameter of the robot's chassis. In order to avoid mobile robot slipping, the actual command velocities (v_R, v_L) of the wheels are bounded by the allowable acceleration. In this work, the maximum allowable acceleration is represents as a_{max}.

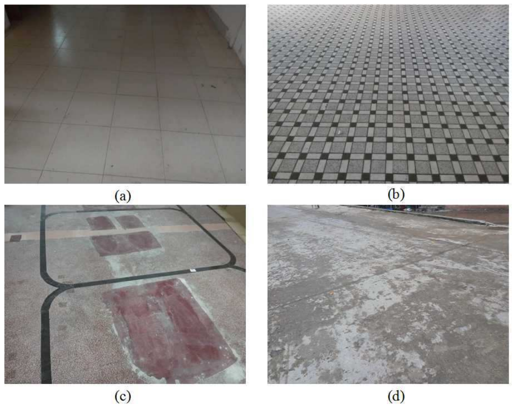

Fig. 5. The various experimental road surface condition. a) smooth ceramic tile floor; b) flat hard road surface; c) rough concrete floor; d) concrete floor with about $10°$ slope.

C. Experiment Results

The parameters are chosen as $R = 0.1I$, $Q = 0.1I$, $N_u = 2$, $N = 3$. The sampling period is $T = 0.1s$. For these two robots, we choose the boundaries of their position x and y and heading angle as $x_{max} = 10$, $y_{max} = 10$, $\theta_{max} = 10$, so the maximum of the states variable are $\xi_{1max} = 10 \times max(\sin\theta - \cos\theta) = 10\sqrt{2}$, $\xi_{2max} = 10 \times max(\cos\theta + \sin\theta) = 10\sqrt{2}$, therefore, the bounded state vectors of system are chosen as $[\bar{x}_{1max}, \bar{\xi}_{max}]^T = [10\ 10 \cdots 10\sqrt{2}]^T \in R^{3N}$, $[\bar{x}_{1min}, \bar{\xi}_{min}] = [-10\ \ -10 \cdots -10\sqrt{2}]^T \in R^{3N}$. And the bounds of two disturbances are chosen as $d_{1max} = 0.05$, $d_{1min} = -0.05$ and $d_{2max} = [0.05, 0.05]^T$, $d_{1min} = [-0.05, -0.05]^T$.

In experiments, the actual boundaries of the linear and angular velocities are $\omega^*_{max} = 0.5rad/s$, $v^*_{max} = 0.5m/s$, where ω^*_{max} and v^*_{max} are also the velocities bounds. Then the boundaries of the input are chosen as $u_{1max} = \omega^*_{max}$, so $\bar{u}_{1max} = [u_{1max} \cdots u_{1max}]^T \in R^{2N_u}$ and $\bar{u}_{1min} = -\bar{u}_{1max}$; $u_{2max} = v^*_{max} + \omega_{max}x_{2max} = 0.5 + 5\sqrt{2} \approx 7.57$, $\bar{u}_{2max} = [u_{2max} \cdots u_{2max}]^T \in R^{2N_u}$ and $\bar{u}_{2min} = -\bar{u}_{2max}$. Then, we choose the a_{max} as $5m/s^2$, so $\Delta u_{1max} = a_{max} \times T/L \approx$

$0.833m/s$ then $\Delta\bar{u}_{1max} = [\Delta u_{1max} \cdots \Delta u_{1max}]^T \in R^{2N_u}$ and $\Delta\bar{u}_{1min} = -\Delta\bar{u}_{1max}$; Δu_{2max} is set as $2m/s$, then $\Delta\bar{u}_{2max} = [\Delta u_{2max} \cdots \Delta u_{2max}]^T \in R^{2N_u}$ and $\Delta\bar{u}_{2min} = -\Delta\bar{u}_{2max}$.

Since the dynamic conditions are affected by the road surface condition, slope angle as well as the payload, we have conducted the experiments using two different robots, e.g., "Rob1" and "Rob2", with different payloads for comparative experiment. In addition, various road conditions such as smooth ceramic tile floor, flat hard road surface, rough concrete floor and sloping road as shown in Fig. 5 are used in the experiment. The initial input vector of the robot is $[\omega(0), v(0)]^T = [0, 0]^T$, while the initial states of each experiment are different.

In the practical application, we can get relative smooth moving trajectories by simply tuning the parameter α, and the tuning criteria depended on the experience of designer accumulated from trial and error in simulation and experiment studies.

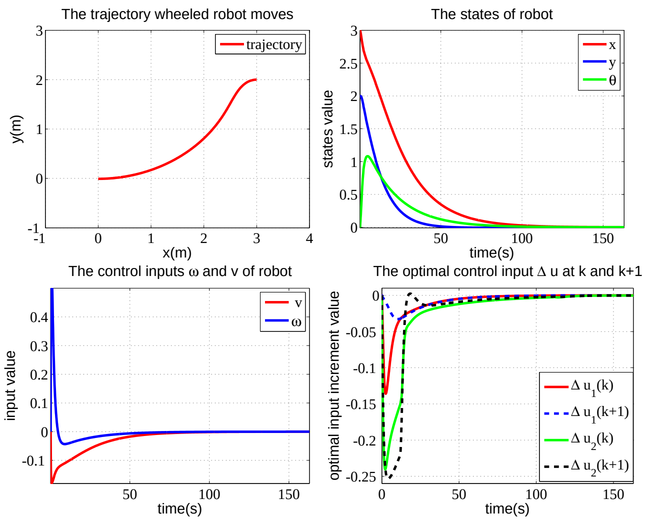

Fig. 6. Rob_1 moving on smooth ceramic tile floor, starting from $(3, 2, 0)$, $\lambda = 1.2$, $\alpha = 0.62$, $\vartheta = 0.1$.

Figs. 6–9 show the four experimental results which include the trajectories of robot, the states, control inputs and the optimal input increments. In experiments, the control parameters can be chosen dependent on the different dynamic condition. From these figures, we can see that, although the dynamic conditions are different in each experiment, the robots are able to approach the origin point eventually. On the other hand, due to the low value of α, there are longer convergent time and higher fluctuation of heading angle θ in Figs. 8–9, so there are relatively sharp transitions in their trajectories. From the figures of states, the robust model predictive control based on primal-dual neural network can stabilize the wheeled robot system successfully despite of the effect of disturbance $d(k)$. Owing to the added exponential decaying term in (8), at the beginning of movement, the angular velocity ω reached a relatively high value, but the velocity bound restrict its value. Finally ω and v both converge to zero.

Remark 6.1: In the experiments, the proposed control method runs on a industrial computer with Inter(R) Pen-

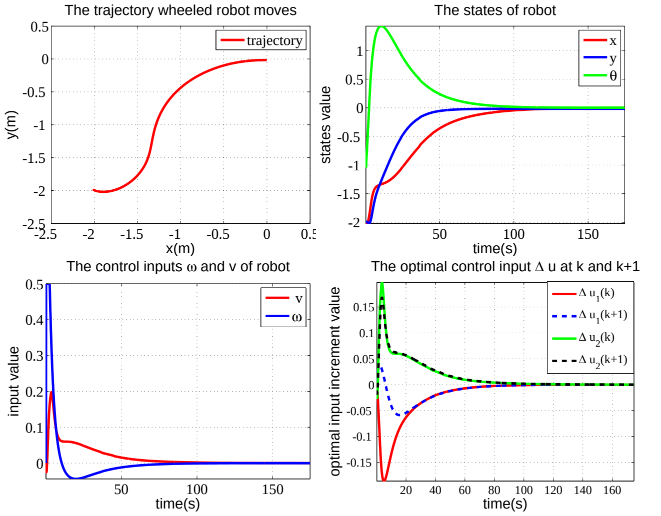

Fig. 7. Rob_2 moving on flat hard road surface, starting from $(-2, -2, -\frac{\pi}{3})$, $\lambda = 1.05$, $\alpha = 0.2$, $\vartheta = 0.1$.

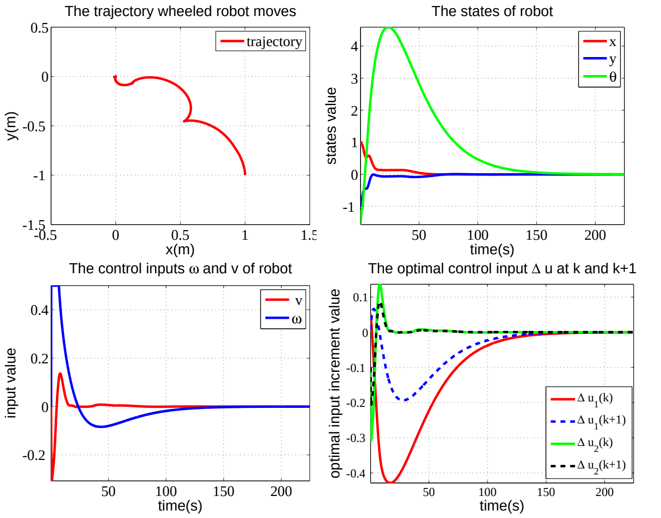

Fig. 8. Rob_2 moving on rough concrete floor, starting from $(1, -1, -\frac{\pi}{2})$, $\lambda = 1.1$, $\alpha = 0.04$, $\vartheta = 0.1$.

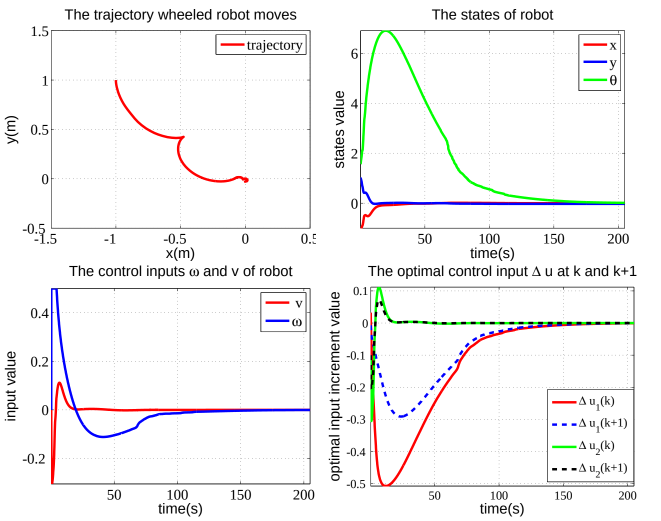

Fig. 9. Rob_1 moving on concrete floor with about $10°$ slope, starting from $(-1, 1, \frac{\pi}{2})$, $\lambda = 1.1$, $\alpha = 0.04$, $\vartheta = 0.1$.

tium(R) E5700 @ 3.00 GHz. The sampling time is chosen as 100ms. During the sample time, the PDNN solving the QP problem of subsystem (6) spends about 0.005s, and the PDNN solving the QP problem of subsystem (7) spends 0.032s. The actual cycling time is 0.062s, which is obviously less than the sampling time. From the above analysis, we can see that the proposed control method can be real-time implemented, and the actual implementation can verify the effectiveness of the proposed approach as well.

VII. Conclusions

In this paper, a robust model predictive control (RMPC) method has been proposed to stabilize our developed mobile robot. Based on the dynamics of the nonholonomic robot system, scaling transformation is applied to formulate the system dynamics into a chained form, and thereafter the dynamics are reorganized into two subsystems. An explicit exponential decaying term was combined to the first subsystem to avoid the vanishing of u_1. Using a primal-dual neural network (PDNN) over a finite receding horizon, the proposed RMPC method iteratively solves a formulated quadratic programming (QP) problem by taking the bounded disturbances into account. The implemented neural networks are stable in the sense of Lyapunov as well as globally convergent to the exact optimal solutions of reformulated convex programming problems. Rigorous analysis has been performed to establish the stability of PDNN and RMPC. Extensive experimental studies have been performed demonstrate that the proposed method can steer the mobile robot satisfactorily approach the original point and stabilize the nonholonomic system.

References

[1] J.-S. Hu, J.-J. Wang, and D. M. Ho, "Design of sensing system and anticipative behavior for human following of mobile robots," *IEEE Trans. Ind. Electron.*, vol. 61, no. 4, pp. 1916–1927, April 2014.

[2] R. Brockett, "Asymptotic stability and feedback stabilization," in *Differential Geometry Control Theory*, (Basel: Birkhauser), pp. 181–208, 1983.

[3] A. Bloch, M. Reyhanoglu, and N. McClamroch, "Control and stabilization of nonholonomic dynamic systems," *IEEE Trans. Automatic Control*, vol. 37, pp. 1746–1757, 1992.

[4] D. Gu and H. Hu, "A stabilizing receding horizon regulator for nonholonomic mobile robots," *IEEE Trans. Robotics*, vol. 21, pp. 1022–1028, 2005.

[5] D. Gu and H. Hu, "Receding horizon tracking control of wheeled mobile robots," *IEEE Trans. Control Systems Technology*, vol. 14, no. 4, pp. 743–749, Jul. 2006.

[6] D. Gu and E. Yang, "A suboptimal model predictive formation control," *IEEE/RSJ International Conference on Intelligent Robots and Systems*, pp. 1295–1300, 2005.

[7] P. Morin and C. Samson, "Control of nonholonomic mobile robots based on the transverse function approach," *IEEE Trans. Robotics*, vol. 25, no. 5, pp. 1058–1073, Oct. 2009.

[8] D. Buccieri, D. Perritaz, P. Mullhaupt, Z.-P. Jiang, and D. Bonvin, "Velocity-scheduling control for a unicycle mobile robot: theory and experiments," *IEEE Trans. Robotics*, vol. 25, no. 2, pp. 451–458, Apr. 2009.

[9] B. Zhou, J. Han, X. Dai, " Backstepping based global exponential stabilization of a tracked mobile robot with slipping perturbation," *Journal of Bionic Engineering*, vol. 8, pp. 69–76, 2011.

[10] H. Chen , C. Wang , Z. Liang , D. Zhang, and H. Zhang, " Robust practical stabilization of nonholonomic mobile robots based on visual servoing feedback with inputs saturation," *Asian Journal of Control*, vol. 16, no. 3, pp. 692–702, May 2014.

[11] M. Yue, G. Wu, S. Wang, and C. An, " Disturbance observer-based trajectory tracking control for nonholonomic wheeled mobile robot subject to saturated velocity constraint," *Applied Artificial Intelligence: An International Journal*, vol. 28, no. 8, pp. 751–765, 2014.

[12] Z. Li, Y. Xia, C.-Y. Su, J. Deng, J. Fu and W. He, "Missile guidance law based on robust model predictive control using neural network optimization," *IEEE Trans. Neural Networks and Learning Systems*, vol. 26, no. 8, pp. 1803–1809, 2015.

[13] A. S. Al-Araji, M. F. Abbod, H. S. Al-Raweshidy, "Design of an adaptive neural predictive nonlinear controller for nonholonomic mobile robot system based on posture identifier in the presence of disturbance," *International Journal of Simulation: Systems, Science and Technology*, vol. 12, no. 3, pp. 17-28, 2011.

[14] M. Michalek, K. Kozlowski, "Vector-field-orientation feedback control method for a differentially driven vehicle," *IEEE Trans. Control Systems Technology*, vol. 18, no. 1, pp. 45–65, 2010.

[15] M. Michalek, M. Kielczewski, " Cascaded VFO set-point control for N-trailers with on-axle hitching," *IEEE Trans. Control Systems Technology*, vol.22, no.4, pp.1597–1606, 2014.

[16] S. Maniatopoulos, D. Panagou and K. J. Kyriakopoulos, " Model predictive control for the navigation of a nonholonomic vehicle with field-of-view constraints" *IEEE Conference on American Control Conference (ACC), 2013*, pp. 3967–3972, 2013

[17] X. Zhang, Y. Fang, X. Liu, "Motion-estimation-based visual servoing of nonholonomic mobile robots," *IEEE Trans. Robotics*, vol. 27, no. 6, pp. 1167–1175, 2011.

[18] C. Samson, "Control of chained systems application to path following and time-varying point-stabilization of mobile robots," *IEEE Trans. Automatic Control*, vol. 40, no. 1, pp. 64–77, 1995.

[19] A. Bemporad, F. Borelli, and M. Morari, "Model predictive control based on linear programming-The explicit solution," *IEEE Trans. Autom. Control*, vol. 47, no. 12, pp. 1974–1985, Dec. 2002.

[20] K. P. Tee and S. S. Ge, "Control of nonlinear systems with full state constraint using a barrier Lyapunov function," in *Proc. 48th Conference on Decision Control*, pp. 967–971, 2009.

[21] F. H. Clarke and R. J. Stern, "State constrained feedback stabilization," *Automatica*, vol. 42, no. 2, pp. 422–441, 2003.

[22] R. J. Stern, "Brockett's stabilization condition under state constraints," *Syst. Control Lett.*, vol. 47, pp. 335–341, 2002.

[23] C. Lu and C. Tsai, "Adaptive predictive control with recurrent neural network for industrial processes: An application to temperature control of a variable-frequency oil-cooling machine" *IEEE Trans. Ind. Electron.*, vol. 55, no. 3, pp. 1366–1375, Mar. 2008.

[24] M. Cychowski, K. Szabat, and T. Orlowska-Kowalska, "Constrained model predictive control of the drive system with mechanical elasticity" *IEEE Trans. Ind. Electron.*, vol. 56, no. 6, pp. 1963–1973, Jun. 2009.

[25] R. X. Cui, Y. Li, W. S. Yan, " Mutual information-based multi-AUV path pPlanning for scalar field sampling using multidimensional RRT,"*IEEE Trans. Systems, Man, and Cybernetics: Systems*, vol. 46, no. 7, pp.993-1004, 2016.

[26] W. He, Y. Dong, C. Sun, "Adaptive neural impedance control of a robotic manipulator with input saturation," *IEEE Trans. Systems, Man, and Cybernetics: Systems*, vol. 46, no. 3, pp. 334-344, 2016.

[27] Y. Zhang, S. S. Ge, and T. H. Lee, "A unified quadratic-programming-based dynamical system approach to joint torque optimization of physically constrained redundant manipulators," *IEEE Trans. System, Man and Cybernetics–Part B*, vol. 34, no. 5, pp. 2126–2132, Oct. 2004.

[28] Z. Li, S. S. Ge, and S. Liu, "Contact-force distribution optimization and control for quadruped robots using both gradient and adaptive neural networks," *IEEE Trans. Neural Networks and Learning Systems*, vol. 25, no. 8, pp. 1460–1473, Aug. 2014.

[29] G. Oriolo, A. Luca, M. Vandittelli, "WMR Control via dynamic feedback linearization: design, implementation, and experimental validation," *IEEE Trans. Control Systems Technology*, vol. 10, no. 6, pp. 835–852, 2002.

[30] D. W. Tank, J. J. Hopfield, "Simple neural optimization networks: an A/D converter, signal decision circuit, and a linear programming circuit," *IEEE Trans. Circuits System*, vol. 33, no. 5, pp. 533–541, 1986.

[31] M. P. Kennedy, L. O. Chua, "Neural networks for nonlinear programming," *IEEE Trans. Circuits System*, vol. 35, no. 5, pp. 554–562, 1988.

[32] M. S. Bazaraa, H. D. Sherali, C. M, Shetty, "Nonlinear programming theory and algorithms (2nd ed.)," *New York: Wiley*, 1993.

[33] W. Li, J. Swetits, "A new algorithm for solving strictly convex quadratic programs," *SIAM Journal on Optimization*, vol. 7, no. 3, pp. 595–619, 1997.

[34] D. P. Bertsekas, *Parallel and distributed computation: numerical methods*, Englewood Cliffs, NJ: Prentice-Hall, 1989.

[35] Z. Li, J. Deng, R. Lu, Y. Xu, J. Bai, C.-Y. Su, "Trajectory track control of mobile robot systems incorporating neural-dynamic optimi model predictive approach," *IEEE Trans. Systems, Man and Cyberneti Systems*, vol. 46, no. 6, pp. 740–749, 2016.
[36] I. Kolmanovsky, N.H. McClamroch, "Developments in nonholonoı control problems," *IEEE Control Systems*, vol.15, no.6, pp. 20–36, 19

Hanzhen Xiao received the B.Eng. degree in College of Automation Science and Engineering, South China Univ. of Tech., Guangzhou, China, in 2013. He is working toward Master Degree in in College of Automation Science and Engineering, South China Univ. of Technology. His research interests are model predictive control, mobile robot, neural network control and optimization.

Zhijun Li (M'07-SM'09) received the Ph.D. deg in mechatronics, Shanghai Jiao Tong University R. China, in 2002. From 2003 to 2005, he wa postdoctoral fellow in Department of Mechani Engineering and Intelligent systems, The University of Electro-Communications, Tokyo, Japan. From 2005 to 2006, he was a research fellow in the Department of Electrical and Computer Engineering, National University of Singapore, and Nanyang Technological University, Singapore. From 2007-2011, he was an Associate Professor in the Department of Automation, Shanghai Jiao Tong University, P. R. China. Since 2012, he is a Professor in College of Automation Science and Engineering, South China university of Technology, Guangzhou, China. From 2016, he is the Chair of Technical Committee on Biomechatronics and Biorobotics Systems (B2S), IEEE Systems, Man and Cybernetics Society. He is serv as an Editor-at-large of Journal of Intelligent & Robotic Systems, Associ Editors of IEEE Transactions on Neural Networks and Learning Syste and IEEE Transactions on Systems, Man and Cybernetics: Systems, IEEE Transactions on Automation Science and Engineering. He has b the General Chair of 2016 IEEE Conference on Advanced Robotics Mechatronics, Macau, China. Dr. Li's current research interests incl service robotics, tele-operation systems, nonlinear control, neural netw optimization, etc.

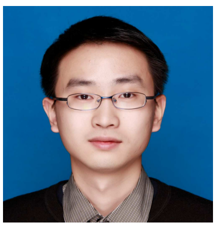

Chenguang Yang (S'07-M'10-SM'16) received B.Eng. degree in measurement and control fr Northwestern Polytechnical University, Xian, Chi in 2005, and the Ph.D. degree in control er neering from the National University of Singapo Singapore, in 2010. He received postdoctoral tra ing at Imperial College London, UK. He is w Zienkiewicz Centre for Computational Engineeri Swansea University, UK as a senior lecturer. is a recipient of the 2011 IEEE Transactions on Robotics Best Paper Award. His research interests lie in robotics, automation and computational intelligence.

Lixian Zhang received the Ph.D. degree in control science and engineering from Harbin Institute of Technology, China, in 2006. From Jan 2007 to Sep 2008, he worked as a postdoctoral fellow in the Dept. Mechanical Engineering at Ecole Polytechnique de Montreal, Canada. He was a visiting professor at Process Systems Engineering Laboratory, Massachusetts Institute of Technology (MIT) during Feb 2012 to March 2013. Since Jan 2009, he has been with the Harbin Institute of Technology, China, where he is currently full professor and vice director in the Research Institute of Intelligent Control and Systems. Dr. Zhang's research interests include nondeterministic switched systems, networked control systems, model predictive control and their applications. He serves as Associated Editors for various peer-reviewed journals including IEEE Transactions on Automatic Control, IEEE Transactions on Cybernetics, etc., and was a leading Guest Editor for a Special Section in IEEE Transactions on Industrial Informatics. He is an IEEE Senior Member and Chair of IEEE SMCS Harbin Section Chapter. He is a Thomson Reuters ISI Highly Cited Researcher in 2014 and 2015. He is a Fellow of IET.

Peijiang Yuan received the B.S. degree in department of automation from the Tsinghua University, Beijing, China, in 1997, and Ph.D. degrees in electronic and computer engineering from University of Western Ontario, Canada, Currently, he is an associate Professor with the Intelligent Technology and Robotics Research Center in Beihang University. His current research interests include aviation manufacturing robot, robot localization and perception, intelligent control and machine vision. Dr. Yuan has served for several international conferences as a Program Committee Member, the Program Committee Co-Chair of the 2010 IEEE World Congress on Computational Intelligence and the committee member of 2011 IEEE Robotics and Automation and Intelligent Robots and Systems.

Liang Ding (S'98- M'10) received the Ph.D. degree in mechanical engineering from the Harbin Institute of Technology, Harbin, China, in 2010. He is currently a Professor with the School of Mechatronics, Harbin Institute of Technology. His current research interests include mechanics, control, and simulation for robotic and mechatronic systems, in particular for planetary exploration rovers and multi-legged robots.

Tianmiao Wang received the B.S degree in Xian Jiaotong University, and the M.S and the Ph.D degrees in the Northwestern Polytechnical University, in 1982, and 1990 respectively. Furthermore, he worked as post-doctoral in State Key Laboratory of Intelligent Technology and Systems of Tsinghua University and the State Bionic Force Laboratory of Italy in 1992,and 1995 respectively. Now, he is the chief of the school of mechanical engineering and automation of the Beijing University of Aeronautics and Astronautics. Prof. Wang is a "Cheung Kong Scholar appointed by Ministry of Education and a member of the Academic Degree Commission of the State Council of China. His research areas are focusing on the mirco-robot technology, medical robot technology and embedded electromechanical control technology.